Polymer 196 (2020) 122479

Contents lists available at ScienceDirect

Polymer

journal homepage: http://www.elsevier.com/locate/polymer

Relaxation behavior of poly(diisopropyl fumarate) including no methylene spacer in the main chain

Yasuhito Suzuki [a,*], Kairi Miyata [b], Masashi Sato [a], Nagisa Tsuji [a], Koji Fukao [b], Akikazu Matsumoto [a,**]

[a] Department of Applied Chemistry, Graduate School of Engineering, Osaka Prefecture University, 1-1 Gakuen-cho, Naka-ku, Sakai, Osaka, 599-8531, Japan
[b] Department of Physics, Ritsumeikan University, 1-1-1 Noji-higashi, Kusatsu, Shiga, 525-8577, Japan

ARTICLE INFO

Keywords:
Glass transition
β relaxation
Dielectric spectroscopy

ABSTRACT

Poly(diisopropyl fumarate) (PDiPF) has dynamic mechanical properties different from the relaxation processes of conventional vinyl polymers, due to the absence of a methylene spacer in the main chain. In this study, we investigated the relaxation behavior of PDiPF using dielectric spectroscopy (DS), differential scanning calorimetry (DSC), wide angle X-ray scattering (WAXS), and dynamic mechanical analysis (DMA). We have demonstrated that the β relaxation of PDiPF has unusual characteristics originating from the absence of a methylene spacer; for example, the β relaxation of PDiPF follows the Vogel–Fulcher–Tammann (VFT) equation, causes a clear step in the DSC curve, and enhances the microscopic packing of the polymer chains in the solid state. These β relaxation behaviors of PDiPF reflect the enlarged cooperative rearranging region (CRR).

1. Introduction

Internal dynamics of polymer chains define their viscoelastic properties [1]. Dynamical behaviors of polymers have been extensively investigated using mechanical spectroscopy [2], dielectric spectroscopy (DS) [3,4], and NMR spectroscopy [5,6]. In particular, the dynamics of polyacrylates and polymethacrylates have been investigated in detail [1]. The molecular dynamics of poly(1,2-substituted ethylene) chains is fundamentally different from those of vinyl polymers due to the absence of a methylene spacer (–CH_2–) in the main chain [7–10]. In many cases, however, the polymerization of 1,2-substituted ethylenes does not proceed because of their extremely slow propagation kinetics. An exception is the polymerization of dialkyl fumarates with a bulky ester group because steric hindrance from the bulky ester group leads to a slow termination rate as well. Only when a subtle balance is achieved between propagation and termination, a high-molecular-weight polyfumarate is produced [7].

In the field of polymer physics, the majority of researches on dynamics have focused on α relaxation processes [3]. Typically, α relaxation is the strongest relaxation process and governs the glass transition [11]. It is empirically known that the dynamics of α relaxation can be well fitted with the Vogel–Fulcher–Tammann (VFT) equation [12]. The calorimetric analysis captures a glass transition temperature (T_g) [13] because the heat capacity changes at T_g. For polymeric materials, α relaxation is attributed to the segmental dynamics of the main chain [1]. The commonly accepted theoretical and practical importance of the glass transition leads to extensive fundamental researches [14,15]. An important area of research is a change in T_g in thin films [16–22]. Several researches have revealed the fastening of α relaxation when the interaction between a thin film and a substrate is not strong [22]. More recent researches captured spatial and temporal heterogeneities at the vicinity of T_g [23,24]. The domain of heterogeneities is considered to be a few nanometers [24].

In contrast to α relaxation, less attention has been devoted to β relaxation [3]. The length scale correlated with β relaxation is much smaller than that of α relaxation. Indeed, β relaxation follows the Arrhenius equation indicating that the length and time scales of β relaxation are smaller than the spatial and temporal heterogeneities [25]. Typically, the intensity of β relaxation determined from mechanical spectroscopy is much smaller than that of α relaxation [2]. A simple view for polymeric materials is to attribute β relaxation to the dynamics of the side chains. While the molecular level understanding of β relaxation is still limited [3], Johari and Goldstein found β relaxation for completely rigid molecules without any flexibility [25,26]. Sometimes,

* Corresponding author.
** Corresponding author.
E-mail addresses: suzuki@chem.osakafu-u.ac.jp (Y. Suzuki), matsumoto@chem.osakafu-u.ac.jp (A. Matsumoto).

https://doi.org/10.1016/j.polymer.2020.122479
Received 26 December 2019; Received in revised form 3 March 2020; Accepted 12 April 2020
Available online 19 April 2020

this type of relaxation is referred to as Johari-Goldstein β relaxation, which describes the relaxation process of glasses and other disordered materials as the universal property. The JG β relaxation is regarded as the precursor of α relaxation, and it facilitates viscous flow before the occurrence of α relaxation. Multidimensional NMR studies of poly(ethyl methacrylate) elucidated the coupling of α and β relaxations [5]. These findings imply that some β relaxation is a local step of α relaxation [6].

Previous researches depicted unique properties of poly(dialkyl fumarate)s [27,28]. The study of poly(diisopropyl fumarate) (PDiPF) showed a strong β relaxation [10]. The storage modulus decreased from ~1 GPa to ~0.1 GPa at the β relaxation temperature. The storage modlus decreased from sloid (~1 GPa) to a soft solid (~0.1 GPa) at the β relaxation temperature (28 °C) and then from a soft solid (~0.1 GPa) to a liquid (below 10 MPa) at the α relaxation temperature (177 °C) [28]. When diisopropyl fumarate (DiPF) is randomly copolymerized with an acrylate, the secondary relaxation from DiPF and the primary relaxation from the acrylate merged as the acrylate composition increases [28]. However, in our previous research, the narrow frequency window limited the understanding of the dynamics of PDiPF [10]. In this study, we investigated the relaxation processes of PDiPF using DS for the purpose of deeper consideration of the unique properties of PDiPF and an expansion to the fundamental interpretation of α and β relaxations. The obtained data by DS are helpful in understanding the experimental results of the dynamic mechanical analysis (DMA) and differential scanning calorimetry (DSC). Wide angle X-ray scattering also captures the unusual characteristics of the PDiPF.

2. Experimental methods

2.1. Materials

DiPF and Diethyl fumarate (DEF) were purchased from Fujifilm Wako Pure Chemical Corporation, Tokyo, Japan. The monomer was distilled under reduced pressure prior to use. Dimethyl 2,2′-azobis(2-methylpropionate) (MAIB, Fujifilm Wako Pure Chemical Corporation, Tokyo, Japan) was purified via recrystallization in hexane before use. PDiPF was prepared by radical polymerization with MAIB and purified by reprecipitation in water/methanol mixture. The purified polymer was dried at 50 °C for 8 h under vacuum. The weight average molecular weight (M_w) of PDiPF was 1.2×10^5 g/mol and polydispersity index (PDI) was 1.3. Poly(methyl methacrylate) (PMMA) ($M_w = 8.2 \times 10^4$ g/mol, PDI = 2.4) was purchased from Sigma Aldrich and used without purification. The M_w and PDI of PDiPF were 9.1×10^4 g/mol and 1.2, respectively. The M_w and PDI of PDEF were 7.6×10^4 g/mol and 1.2, respectively.

2.2. Dynamic mechanical analysis (DMA)

The samples for DMA measurements were prepared by thermal welding. Approximately 1.5 g of the polymer was inserted in a rectangular mold (5 cm × 1 cm). After the polymer was annealed for 30 min at 200 °C, the pressure (approximately 1 MPa) was applied for 1 h at the same temperature. A rectangular sample with a thickness of 2 mm was obtained. The surface was smoothened using a sand paper. DMS 6100 (Seiko Instruments Inc., Tokyo, Japan) was utilized for the DMA. The condition was a dual cantilever mode with a heating rate of 2 °C/min. Sinusoidal strains with an amplitude of 10 μm at 10, 5, 2, 1 and 0.5 Hz were applied.

2.3. Dielectric spectroscopy (DS)

The sample for DS measurements was prepared by solution casting from the toluene solution of PDiPF. The film thickness was approximately 25 μm. DS measurements were carried out using an impedance analyzer (Novocontrol AKB analyzer) in a temperature range from 0 °C to 220 °C with a frequency range from 0.01 Hz to 2 MHz. The complex dielectric permittivity $\varepsilon^* = \varepsilon' - i\varepsilon''$ was obtained as functions of frequency and temperature. The empirical equation of Havriliak and Negami was used to analyze the α, β, and γ relaxation processes [29,30].

$$\varepsilon^*(\omega) = \varepsilon_\infty + \Sigma \frac{\Delta\varepsilon}{[1 + (i\omega\tau)^M]^N} \quad (1)$$

where ε_∞ is the dielectric permittivity at the high frequency limit, $\Delta\varepsilon$ is the dielectric strength, M and N are the shape parameters, and τ is the relaxation time.

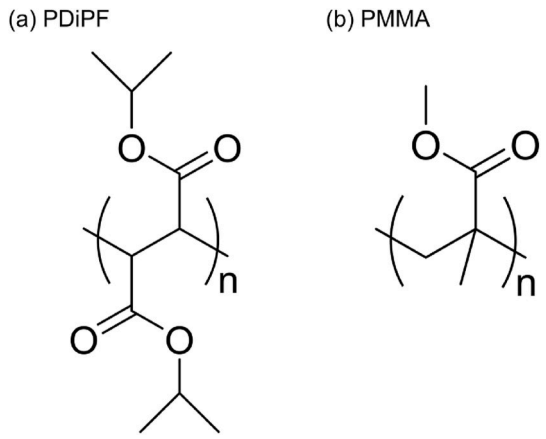

Scheme 1. Schematics of PDiPF and PMMA.

2.4. Wide angle X-ray scattering (WAXS)

In-situ X-ray scattering measurements were conducted at the BL40B2 beamline of SPring-8 (Japan Synchrotron Radiation Research Institute, Hyogo, Japan). Approximately 3 mg of sample was sealed in a sample holder with Capton films (50 μm) for both sides. The sample was mounted on a heating stage (Linkam Scientific Instruments Ltd, Waterfield, England). The sample was heated from 0 °C to 120 °C and then cooled from 120 °C to 0 °C with a scanning rate of 10 °C/min. The wavelength (λ) of the synchrotron beam was 1.00 Å. A flat panel detector (C9728DK, Hamamatsu Photonics K.K., Shizuoka, Japan) was used. The camera distance from the sample was 85.446 mm. During the heating, the X-ray was exposed for 1 s every 6 s. The 2D image was analyzed using a software Fit2D (ESRF).

3. Results and discussion

The structure of PDiPF is shown in Scheme 1. As a comparison, the structure of PMMA is also shown. The significant feature of PDiPF is the absence of methylene spacer in the main chain. Polymers originating from monosubstituted ethylene or 1,1-disubstituted ethylene including MMA have methylene spacer in the main chain. With respect to the bond length of two carbons, the bulkiness of the side chains of DiPF is captured.

Fig. 1 (a) shows a DMA curve for PDiPF measured at 10, 5, 2, 1, and 0.5 Hz with a scanning rate of 2 °C/min from room temperature to 250 °C. As an intense peak was observed at 87 °C at 2 Hz in tan δ, the storage modulus (E') decreased from 1.1 GPa at 40 °C to 0.13 GPa at 120 °C. At a higher temperature approximately 220 °C, a small peak is observed. The data are in good agreement with literature [10]. The measurement was stopped at 250 °C because decomposition starts around the temperature [10,28]. As the reference polymer, Fig. 1 (b) displays the DMA curve of PMMA measured at the same instrument from −20 °C to 150 °C. At 114 °C, a single relaxation process is observed. The storage modulus decreased from 1.46 GPa at 80 °C to 2.3 MPa at 140 °C. Above 150 °C, the polymer becomes too soft to continue the measurement. The

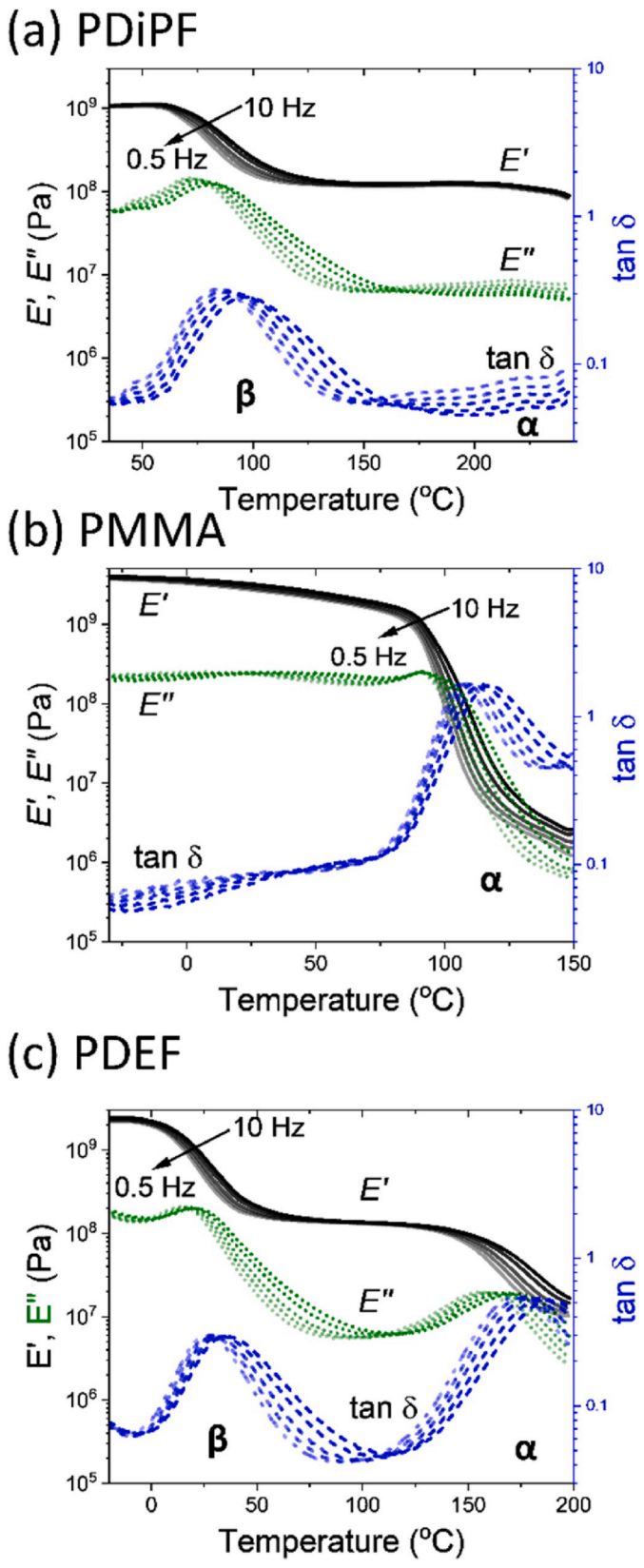

Fig. 1. Dynamic mechanical analysis of (a) PDiPF and (b) PMMA, and (c) PDEF measured at 10, 5, 2, 1, and 0.5 Hz displayed from darker color to lighter color as indicated as an arrow. The storage modulus, the loss modulus, and tan δ are shown in black line, green dot line, and blue dash line, respectively. (For interpretation of the references to color in this figure legend, the reader is referred to the Web version of this article.)

relaxation process is attributed to the segmental dynamics of the main chain (α relaxation process).

Above the T_g, the storage modulus either simply decrease or shows a plateau depending on the molecular weight. The plateau appears when the molecular weight is higher than the entanglement molecular weight (M_e) and is called a rubbery plateau. The storage modulus (E') of the rubbery plateau is calculated from the following equation [31].

$$E' = \frac{2(1+\mu)\rho RT}{M_e} \tag{2}$$

Here, μ is the poisons ratio. Generally, polymers have storage modulus of ca. 10^5 Pa at a rubbery plateau and this is the case for PMMA as well [32]. Although there is a β relaxation process that corresponds to the side-chain relaxation at a lower temperature [2], the effect on the mechanical properties is very small. The temperatures of the α and β relaxation shift significantly depending on the ester alkyl groups in the side chain and in the presence or absence of the α-methyl substituent on the main chain [33]. Nevertheless, both polyacrylates and polymethacrylates have qualitatively similar DMA curves [1].

In contrast to the DMA results of PMMA and other poly(meth)acrylates, the DMA curve of PDiPF is fundamentally different. There is a plateau region in between the two relaxations at 71 °C and 220 °C. Given that the storage modulus is ca. 0.12 GPa below 180 °C, this is not the rubbery plateau. According to the equation (2), the storage modulus of most polymers at rubbery plateau are expected to be the order of 10^5 Pa or less depending on the entangle molecular weights [34]. The storage modulus of ca. 0.12 GPa means that PDiPF is still a solid rather than a polymer melt. In other words, the relaxation process at 71 °C is not the segmental dynamics. As is discussed later, we assigned this relaxation process as β relaxation, although this process shows unusual behaviors. The higher relaxation process is attributed to α relaxation. This assignment is supported by the data from PDEF as shown in Fig. 1 (c). PDEF shows qualitatively similar DMA behavior. In addition, the α relaxation of PDEF is clearly observed. The α relaxation temperature for PDEF was lower than that of PDiPF, due to the decrease in the steric bulkiness of the ester alkyl group.

In order to elucidate the relaxation behavior of PDiPF for a broad frequency range, dielectric relaxation spectroscopy was applied. Selected dielectric loss curves were plotted in Fig. 2. There were three distinct processes. The spectra were fitted with the Havriliak-Negami function [29,30]. The temperature-frequency plot of these processes is summarized in Fig. 3. In most cases, only the α relaxation process follows the VFT equation [12]:

$$\tau = \tau_0 exp\left(\frac{U}{T - T_0}\right) \tag{3}$$

where τ_0 is the relaxation time at high temperature limit, U is a constant, and T_0 is the Vogel temperature. These three processes depicted in Fig. 2 are assigned as α, β, and γ processes from the slowest process. Here, the γ process follows the Arrhenius equation. The activation energy was 25 kJ/mol. Significantly, the β relaxation process follows the VFT equation in the case of PDiPF. As is the same as other polymers, the α relaxation process follows the VFT equation as well.

The glass transition occurs when the size of the cooperative rearranging region (CRR) [35,36] is on the order of few nanometers though the details are still under debate [11]. In general, the β relaxation process follows the Arrhenius equation because the CRR is smaller than the critical size for the glass transition. The detailed relaxation analysis by NMR showed that the molecular origin of the β relaxation process of PMMA arose from the side chain flip whose motion was accompanied with the main chain rearrangement [6]. This was consistent with the view that the β relaxation process was regarded as a local step of the α relaxation process [3]. In the case of PDiPF, the constraints of the rotational motion due to the bulky side groups may increase the CRR region of the β relaxation process. Provided that the α and β relaxation

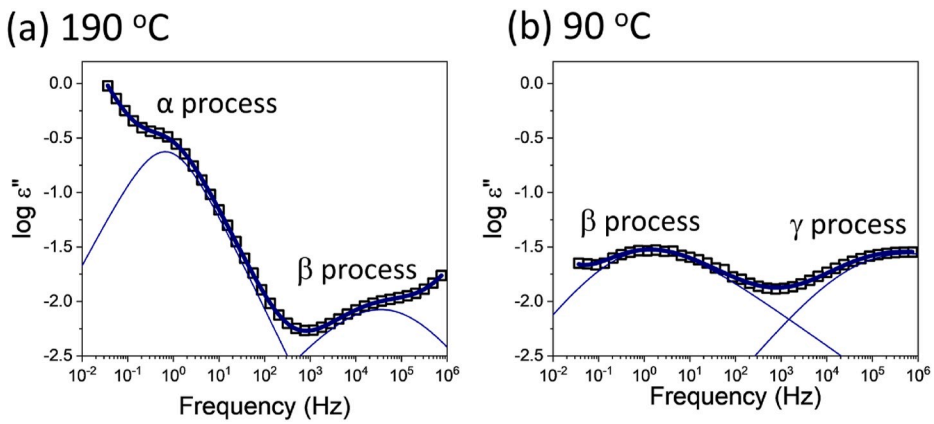

Fig. 2. Selected dielectric loss curves of PDiPF measured at (a) 190 °C and (b) 90 °C. The data point (empty square) and fittings (blue) are displayed. The spectra were fitted with the Havriliak-Negami function. (For interpretation of the references to color in this figure legend, the reader is referred to the Web version of this article.)

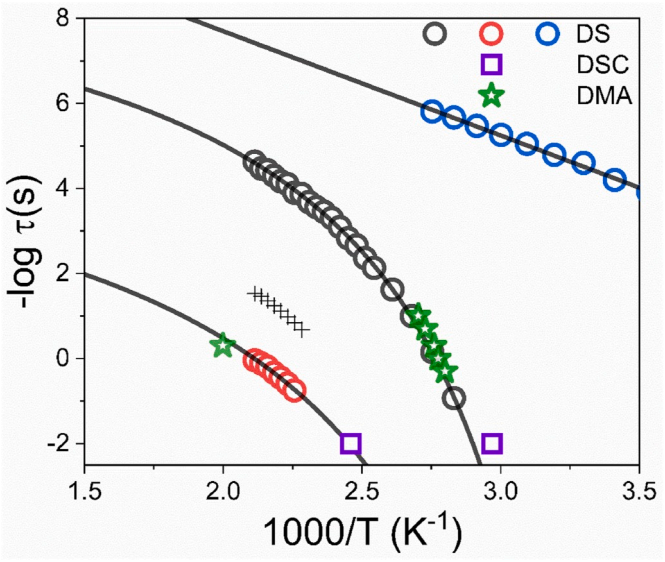

Fig. 3. Relaxation times at maximum loss corresponding to the α-process (red), the β-process (gray), and the γ-process (blue) of PDiPF. Both α- and β-processes were fitted with the VFT equation. The circles, squares, and stars indicate the data obatined by DS, DSC, and DMA measuremnets, respectively. The black crosses indicate the $\tau_{0,CM}$ based on coupling model. (For interpretation of the references to color in this figure legend, the reader is referred to the Web version of this article.)

Table 2
The VFT fitting parameters for the α and β relaxation processes of PDiPF.

	U (K)	T_0 (K)	τ_0 (s)
α process	691.7	276.5	7.65×10^{-9}
β process	788.1	276.5[a]	9.99×10^{-5}

[a] The value was fixed.

are intimately related, it is reasonable to assume that the transition processes have the single ideal glass temperature (T_0). Using the VFT equation, we fit the α and β relaxation with the parameters listed in Table 2. The T_0 of the α relaxation was fixed. The fit is shown in Fig. 3 with gray lines. In this fit, it was assumed that α and β relaxations merge at a low temperature (glassy state). In other words, they have the same Vogel temperature. We let the other parameters free for the fitting. As a result, the τ_0 of α and β relaxations are different. It is known that in many

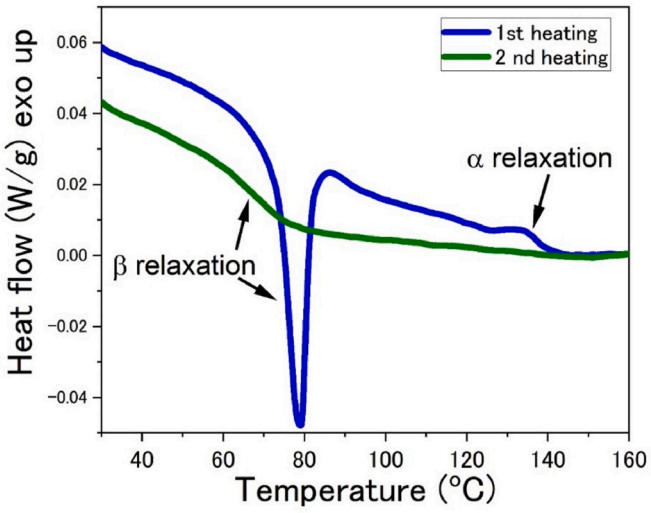

Fig. 4. Calorimetric data of PDiPF on heating at a scanning rate of 10 °C/min. The first heating (blue) and the second heating (green) are displayed. (For interpretation of the references to color in this figure legend, the reader is referred to the Web version of this article.)

polymers, α and β relaxation merge at a high temperature limit [37]. Thus, another scenario is possible. In Fig. S1, we include fitting with fixed T_0 and τ_0. These fitting parameters are summarized in Table S1. The fit is not as good as the one presented in Fig. 3. The green stars correspond to the DMA data obtained from tan δ. They are in good agreement with the DS data. Recently, dielectric spectroscopy analysis of unsaturated fatty acid captured three VFT dependent relaxation processes. They attribute the unique feature to the inability of side groups to pack efficiently [38]. We further analyzed the DS data according to the methods based on the coupling model with the aim to compare the β relxation of PDiPF to the Johari-Goldstein β relxation. The coupling model predicts the primitive relaxation time ($\tau_{0,CM}$) as follows.

$$\tau_{0,CM} = (\tau_c)^n (\tau_\alpha)^{1-n} \quad (4)$$

Here, τ_c is the crossover time which has the approximate value of 2×10^{-12} s for common polymeric glass-formers [39,40]. The coupling parameter (n) can be calculated from the fitting parameter of Havriliak and Negami equation by the following relation [41].

$$MN = (1-n)^{1.23} \quad (5)$$

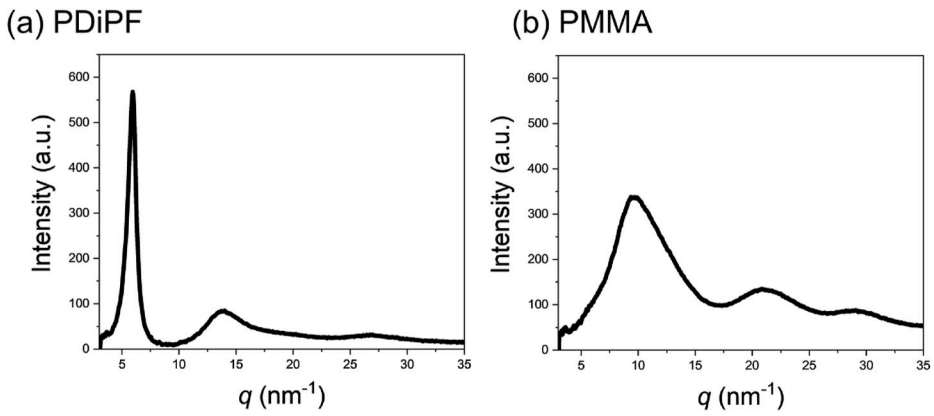

Fig. 5. Wide angle X-ray scattering of (a) PDiPF and (b) PMMA measured at 25 °C. PDiPF shows a sharp amorphous hallo in the low q range.

Ngai et al. found that the $\tau_{0,MCT}$ and the Johari-Goldstein β relaxation time are approximately the same. In Fig. 3, we include the $\tau_{0,CM}$ as black crosses. It seems $\tau_{0,CM}$ and β relaxation are different. In addition, the temperature dependence of the dielectric strength of β relaxation is plotted in Fig. S2. The value $T\Delta\varepsilon_\beta$ is plotted against T. According to the Onsager-Kirkwood-Fröhlich approach, $T\Delta\varepsilon_\beta$ is constant for the case of independent dipoles [42]. Some previous research mentions that the intensity of Johari-Goldstein β relaxation increases as the temperature increase. However, the strength of β relaxation decreases as the temperature increases in the case of PDiPF. This could be due to the local packing of PDiPF as we will discuss later with respect to Fig. 6. The similar temperature dependence of dielectric strength is also reported in other molecules [43]. Based on these properties, it seems the β relaxation of PDiPF cannot be categorized as Johari-Goldstein β relaxation in a strict sense. Nevertheless, this point requires further systematic investigation with rigorous fitting.

Fig. 4 shows the results for the DSC measurements of PDiPF at a scanning rate of 10 °C/min. From the first heating, there is an endothermic peak at 79 °C and a weak step at 137 °C. The second heating is utterly different. A clear step was solely observed at 67 °C. From the second heating, there is no indication of the higher temperature relaxation at least with the experimental resolution. It is known that the DSC measurement with a scanning rate of 10 °C/min corresponds to the angular frequency of 10^{-2} Hz [24]. The high and low temperatures obtained from the first heating curve are plotted in Fig. 3. They are consistent with the α and β relaxations of PDiPF, respectively. DSC detects the stepwise change of heat capacity. In most cases, only the α relaxation shows a detectable change of heat capacity. However, the precise measurement of heat can detect β relaxation as well [44–46]. Both α and β relaxations of PDiPF follow the VFT equation. Heat capacity may change at two temperatures corresponding to these two relaxations. The first heating reflects the sample history [47], including the purification process and the annealing conditions. Following the first cooling with 10 °C/min, the second heating only shows a clear step corresponding to the β relaxation. A better packing after the initial heating may be the reason why the heat capacity change at the α process is hidden upon second heating. These results indicate that the sample is sensitive to thermal history. We measured DSC in the temperature range from 2 °C/min to 50 °C/min, but no significant change was observed. A faster temperature change is required to affect the thermal properties of PDiPF.

The β relaxation of PDiPF followed the VFT equation and showed a step in the DSC measurement. The β relaxation of PDiPF looks like to behave as the glass transition at first glance, but it is of completely different nature in truth. This strong β relaxation is the unique feature of PDiPF. Although it is quite rare, there are some reports which detect β relaxation using calorimetry [44,45]. For example, the β relaxation of *o*-terphenyl [45], isopropylbenzene [48], and propylene carbonate [46] have been reported by a precise heat capacity measurement using adiabatic calorimeters. However, the β relaxation followed the Arrhenius equation rather than the VFT equation in the latter cases, unlike the case of PDiPF. Another example of double glass transition is from polymer blends. When two polymers are immiscible, they show distinctly different two T_gs [49,50], which originate from two different polymers. It is noted that double T_gs were also observed for homopolymers under confinement [49,51,52]. Because the confined environment enhances heterogeneity, two layers with distinctly different T_gs appeared. Presumably, these two layers were near the wall and around the center [51]. The authors also reported the effect of the heating speed and the annealing time on the double T_gs. While two distinct T_gs were observed with a slow heating, only a single relaxation was observed with a fast heating [51]. This type of double glass transition phenomenon may have some similarity with the dynamics of PDiPF. In the case of PDiPF, the rotational hindrance may enlarge the length scale of the CRR corresponding to the β relaxation. As a result, the β relaxation starts to behave like another glass transition. Same as the confined polymers, the intensity of the two T_gs depends on the sample history and the heating speed. It is emphasized that PDiPF intrinsically has the two VFT dependent relaxations in the homopolymer without any confining media.

Wide angle X-ray scattering of PDiPF and PMMA were displayed in Fig. 5. Both PDiPF and PMMA are amorphous polymers. At present, the structural origin of the vitrification phenomena is still unclear [24]. Nevertheless, the WAXS data provides information about the correlation length [53,54]. Despite the fact that the structure is amorphous, there is a sharp and a narrow peak from PDiPF at $q = 5.94$ nm^{-1}(Fig. 5 (a)). This is emphasized by comparing the scattering patterns from PMMA shown in Fig. 5 (b). The peak position corresponds to a distance of 1.06 nm. This value is comparable to the cross-sectional diameter of the PDiPF chain. Due to the rotational hindrance, the structure of PDiPF is rigid [55]. This rigidity could be the origin of the preferred chain packing of the PDiPF. A similar low q peak is observed when an organic glass is a vapor deposited in an anisotropic structure [56]. Fig. 6 (a) depicts the temperature dependence of the WAXS peaks of the PDiPF, focusing on the low q peak. The change of the intensity and the q are plotted in Fig. 6 (b). As temperature rises, the intensity becomes higher, and the q value is decreased. While the change of q range on heating is due to the thermal expansion, the change of the intensity reflects the rearrangement of the molecules. The increase of the intensity starts at around 60 °C, which is around the β relaxation temperature. At this temperature, the segmental motion (α relaxation process) is still frozen. Because of the unusually strong β relaxation process, the local motion promotes the rearrangement into a thermodynamically more stable state. In the same plot in Fig. 6 (b), the results on cooling are also plotted. While the q values at the peak maximum are almost the same on heating and cooling, the intensity stays much higher on cooling. In

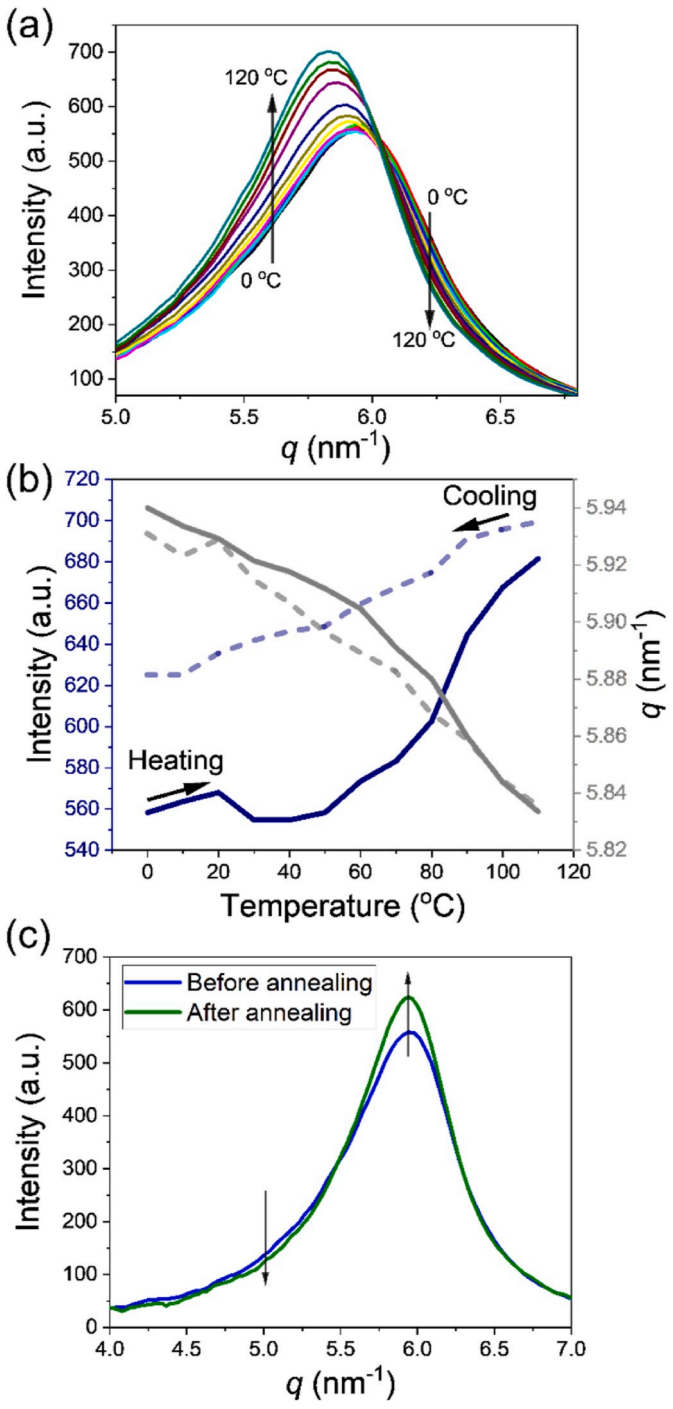

Fig. 6. (a) Wide angle X-ray scattering (WAXS) of PDiPF measured at different temperatures. The data were collected every 10 °C on heating from 0 °C to 120 °C. The low angle amorphous hallow is magnified. (b) The maximum intensity and the peak position as a function of temperature. The blue and gray curves indicate the intensity and q value, respectively. The line and the dotted line represent the heating and the cooling. (c) Comparison of the WAXS profiles at 0 °C before and after the annealing. (For interpretation of the references to color in this figure legend, the reader is referred to the Web version of this article.)

addition, the X-ray profiles at 0 °C before and after the annealing is shown in Fig. 6 (c). After annealing the maximum intensity becomes higher and the peak width becomes narrower. This indicates that the structures before annealing and after annealing are different, in that the structure of the latter is more homogeneous in a thermodynamically more stable state. This irreversible change of the state upon first annealing is consistent with the DSC results. Upon first heating, the broad distribution of the thermodynamic state shows clear heat capacity changes at both β relaxation and α relaxation temperatures. After the first heating, the polymers chains become more thermodynamically stable. Consequently, they mainly respond at the β relaxation on DSC measurement.

4. Conclusion

The molecular dynamics and the structure of PDiPF in the solid state were investigated in this study. The absence of a methylene spacer fundamentally affects the characteristics of the β relaxation of PDiPF. The β relaxation of PDiPF looks like to have some similarity with glass transition for common vinyl polymers including PMMA and other poly (meth)acrylates. The β relaxation time of PDiPF followed the VFT equation rather than the Arrhenius equation. The DSC measurement showed a step from the heat flow curve corresponding to the β relaxation temperature. On the other hand, there are some differences between the β relaxation of PDiPF and conventional glass transition behavior. The DMA, DS, and DSC data indicated that there exists another relaxation at a higher temperature. Unlike the glass transition behavior, the packing structure of the PDiPF chains is more thermodynamically organized during annealing at a temperature above the β relaxation. These unique features presumably originate from the exceptionally large characteristic length of the β relaxation due to the absence of a methylene spacer in addition to the intrinsic rigid chain characteristics of PDiPF.

Declaration of competing interest

The authors declare no conflict of interest.

CRediT authorship contribution statement

Yasuhito Suzuki: Conceptualization, Visualization, Supervision, Writing - original draft. **Kairi Miyata:** Validation, Formal analysis. **Masashi Sato:** Validation. **Nagisa Tsuji:** Validation, Visualization. **Koji Fukao:** Validation, Supervision, Formal analysis. **Akikazu Matsumoto:** Conceptualization, Supervision, Writing - review & editing.

Acknowledgments

The synchrotron radiation experiments were performed at the BL40B2 of SPring-8 with the approval of the Japan Synchrotron Radiation Research Institute (JASRI) (Proposals No. 2018B1141). The authors acknowledge experimental support from Dr. Noboru Ohta and Dr. Hiroshi Sekiguchi at SPring-8.

Appendix A. Supplementary data

Supplementary data to this article can be found online at https://doi.org/10.1016/j.polymer.2020.122479.

References

[1] N.G. McCrum, B.E. Read, G. Williams, Anelastic and Dielectric Effects in Polymeric Solids, Wiley, New York, 1967.
[2] E. Muzeau, J. Perez, G.P. Johari, Mechanical spectrometry of the β-relaxation in poly(methyl methacrylate), Macromolecules 24 (1991) 4713–4723.
[3] K.L. Ngai, M. Paluch, Classification of secondary relaxation in glass-formers based on dynamic properties, J. Chem. Phys. 120 (2004) 857–873.
[4] K.L. Ngai, T.R. Gopalakrishnan, M. Beiner, Relaxation in poly(alkyl methacrylate)s: change of intermolecular coupling with molecular structure, tacticity, molecular weight, copolymerization, crosslinking, and nanoconfinement, Polymer 47 (2006) 7222–7230.
[5] A.S. Kulik, H.W. Beckham, K. Schmidt-Rohr, D. Radloff, U. Pawelzik, C. Boeffel, H. W. Spiess, Coupling of α and β processes in poly(ethyl methacrylate) investigated by multidimensional NMR, Macromolecules 27 (1994) 4746–4754.
[6] K. Schmidt-Rohr, A.S. Kulik, H.W. Beckham, A. Ohlemacher, U. Pawelzik, C. Boeffel, H.W. Spiess, Molecular nature of the β relaxation in poly(methyl

methacrylate) investigated by multidimensional NMR, Macromolecules 27 (1994) 4733–4745.
[7] A. Matsumoto, T. Otsu, Detailed mechanism of radical high polymerization of sterically hindered dialkyl fumarates, Macromol. Symp. 98 (1995) 139–152.
[8] A. Matsumoto, T. Tarui, T. Otsu, Dilute solution properties of semiflexible poly (substituted methylenes): intrinsic viscosity of poly(diisopropyl fumarate) in benzene, Macromolecules 23 (1990) 5102–5105.
[9] H. Kurosu, T. Yamada, I. Ando, K. Sato, T. Otsu, An NMR study of structure and dynamics of poly(fumarate)s in the solid state, J. Molecul. Struc. 300 (1993) 303–311.
[10] K. Yamada, M. Takayanagi, Y. Murata, Relations between molecular aggregation state and mechanical properties in poly(diisopropyl fumarate), Polymer 27 (1986) 1054–1057.
[11] C.A. Angell, Spectroscopy simulation and scattering, and the medium range order problem in glass, J. Non-Cryst. Solids 73 (1985) 1–17.
[12] L.S. Garca-Coln, L.F. Del Castillo, P. Goldstein, Theoretical basis for the vogel-fulcher-tammann equation, Phys. Rev. B 40 (1989) 7040–7044.
[13] J. Rieger, Glass transition temperature T_g of polymers - comparison of the values from differential thermal analysis (DTA, DSC) and dynamic mechanical measurements (torsion pendulum), Polym. Test. 20 (2001) 199–204.
[14] C.A. Angell, The old problems of glass and the glass transition, and the many new twists, Proc. Natl. Acad. Sci. Unit. States Am. 92 (2006) 6675–6682.
[15] C.A. Angell, The glass transition, Curr. Opin. Solid State Mater. Sci. 1 (1996) 578–585.
[16] J.L. Keddie, R.A.L. Jones, R.A. Cory, Interface and surface effects on the glass-transition temperature in thin polymer films, Faraday Discuss 98 (1994) 219–230.
[17] T. Kajiyama, K. Tanaka, A. Takahara, Surface molcular motion of the monodisperse polystyrene films, Macromolecules 30 (1997) 280–285.
[18] J.A. Forrest, K. Dalnoki-Veress, J.R. Dutcher, Interface and chain confinement effects on the glass transition temperature of thin polymer films, Phys. Rev. E 56 (1997) 5705–5715.
[19] K. Fukao, Y. Miyamoto, Glass transitions and dynamics in thin polymer films: dielectric relaxation of thin films of polystyrene, Phys. Rev. E 61 (2000) 1743–1754.
[20] C.J. Ellison, J.M. Torkelson, The distribution of glass-transition temperatures in nanoscopically confined glass formers, Nat. Mater. 2 (2003) 695–700.
[21] R.D. Priestley, C.J. Ellison, L.J. Broadbelt, J.M. Torkelson, Structural relaxation of polymer glasses at surfaces, interfaces, and in between, Science 309 (2005) 456–460.
[22] S. Napolitano, E. Glynos, N.B. Tito, Glass transition of polymers in bulk, confined geometries, and near interfaces, Rep. Prog. Phys. 80 (2017), 036602.
[23] M.D. Ediger, C.A. Angell, S.R. Nagel, Supercooled liquids and glasses, J. Phys. Chem. 100 (1996) 13200–13212.
[24] M.D. Ediger, Spatially heterogeneous dynamics in supercooled liquids, Annu. Rev. Phys. Chem. 51 (2000) 99–128.
[25] G.P. Johari, Glass transition and secondary relaxations in molecular liquids and crystals, Ann. NY Acad. Sci. 279 (1976) 117–140.
[26] G.P. Johari, M. Goldstein, Molecular mobility in simple glasses, J. Phys. Chem. 74 (1970) 2034–2035.
[27] A. Matsumoto, T. Sumihara, Thermal and mechanical properties of random copolymers of diisopropyl fumarate with 1-adamantyl and bornyl acrylates with high glass transition temperatures, J. Polym. Sci. Part A Polym. Chem. 55 (2017) 288–296.
[28] Y. Suzuki, T. Tsujimura, K. Funamoto, A. Matsumoto, Relaxation behavior of random copolymers containing rigid fumarate and flexible acrylate segments by dynamic mechanical analysis, Polym. J. 51 (2019) 1163–1172.
[29] S. Havriliak, S. Negami, A complex plane representation of dielectric and mechanical relaxation processes in some polymers, Polymer 8 (1967) 161–210.
[30] F. Kremer, A. Schönhals, Broadband Dienectric Spectroscopy, Springer-verlag, Berlin, Heidelberg, 2003.
[31] C.P. Hiemenz, P.T. Lodge, Polyme Chemistry, second ed., CRC Press, New York, 2007.
[32] K. Fuchs, C. Friedrich, J. Weese, Viscoelastic properties of narrow-distribution poly (methyl methacrylates), Macromolecules 29 (1996) 5893–5901.
[33] J. Brandrup, E.H. Immergut, E.A. Grulke, Polymer Handbook, fourth ed., Wiley, New York, 2003.
[34] M. Rubinstein, R.H. Colby, Polymer Physics, Oxford University Press, New York, 2003.
[35] G. Adam, J.H. Gibbs, On the temperature dependence of cooperative relaxation properties in glass-forming liquids, J. Chem. Phys. 43 (1965) 139–146.
[36] K.L. Ngai, R.W. Rendell, D.J. Plazek, Couplings between the cooperatively rearranging regions of the adam-gibbs theory of relaxations in glass-forming liquids, J. Chem. Phys. 94 (1991) 3018–3029.
[37] A. Arbe, D. Richter, J. Colmenero, B. Farago, Merging of the a and b relaxations in polybutadiene: a neutron spin echo and dielectric study, Phys. Rev. E 54 (1996) 3853–3869.
[38] A. Pipertzis, A. Hess, P. Weis, G. Papamokos, K. Koynov, S. Wu, G. Floudas, Multiple segmental processes in polymers with cis and trans stereoregular configurations, ACS Macro Lett. 7 (2018) 11–15.
[39] K.L. Ngai, An extended coupling model description of the evolution of dynamics with time in supercooled liquids and ionic conductors, J. Phys. Condens. Matter 15 (2003) S1107–S1125.
[40] J. Colmenero, A. Arbe, G. Coddens, B. Frick, C. Mijangos, H. Reinecke, Crossover from independent to cooperative segmental dynamics in polymers: experimental realization in poly(vinyl chloride), Phys. Rev. Lett. 78 (1997) 1928–1931.
[41] F. Alvarez, A. Alegrıa, J. Colmenero, Relationship between the time-domain Kohlrausch-Williams-Watts and frequency-domain Havriliak-Negami relaxation functions, Phys. Rev. B 44 (1991) 7306–7312.
[42] P.K. Dixon, Specific-heat spectroscopy and dielectric susceptibility measurements of salol at the glass transition, Phys. Rev. B 42 (1990) 8179–8186.
[43] A. Shönhals, F. Kremer, A. Hofmann, E.W. Fischer, E. Schlosser, Anomalies in the scaling of the dielectric α-relaxation, Phys. Rev. Lett. 70 (1993) 3459–3462.
[44] T. Hikima, M. Hanaya, M. Oguni, β-Molecular rearrangement process, but not an α-process, as governing the homogeneous crystal-nucleation rate in a supercooled liquid, Bull. Chem. Soc. Jpn. 69 (1996) 1863–1868.
[45] H. Fujimori, M. Oguni, Correlation index $(T_{g\alpha}\text{-}T_{g\beta})/T_{g\alpha}$ and activation energy ration $\Delta\varepsilon_{a\alpha}/\Delta\varepsilon_{a\beta}$ as parameters characterizing the structure of liquid and glass, *Solid State Commun* 94 (1995) 157–162.
[46] H. Fujimori, M. Oguni, Calorimetric study of D, L-propene carbonate: observation of the β- as well as α-glass transition in the supercooled liquid, J. Chem. Therm. (1994) 367–378.
[47] M.K. Haque, K. Kawai, T. Suzuki, Glass transition and enthalpy relaxation of amorphous lactose glass, Carbohydr. Res. 341 (2006) 1884–1889.
[48] K. Kishimoto, H. Suga, S. Seki, Calorimetric study of the glassy state. VIII. Heat capacity and relaxational phenomena of isopropylbenzene, Bull. Chem. Soc. Jpn. 46 (1973) 3020–3031.
[49] L. Chen, K. Zheng, X. Tian, K. Hu, R. Wang, C. Liu, Y. Li, P. Cui, Double glass transitions and interfacial immobilized layer in in-situ-synthesized polyvinyl alcohol/silica nanocomposites, Macromolecules 43 (2010) 1076–1082.
[50] J. Qiu, C. Xing, X. Cao, H. Wang, L. Wang, L. Zhao, Y. Li, Miscibility and double glass transition temperature depression of poly(L-lactic acid) (PLLA)/Poly (oxymethylene) (POM) blends, Macromolecules 46 (2013) 5806–5814.
[51] L. Li, D. Zhou, D. Huang, G. Xue, Double glass transition temperatures of poly (methyl methacrylate) confined in alumina nanotube templates, Macromolecules 47 (2014) 297–303.
[52] G. Tsagaropoulos, A. Eisenberg, Dynamic mechanical study of the factors affecting the two glass transition behavior of filled polymers. Similarities and differences with random ionomers, Macromolecules 28 (1995) 6067–6077.
[53] R. Lovell, G.R. Mitchell, A.H. Windle, Wide-angle X-ray scattering study of structural parameters in non-crystalline polymers, Faraday Discuss. Chem. Soc. 68 (1979) 46–57.
[54] G.R. Mitchell, A.H. Windle, Structure of polystyrene glasses, Polymer 25 (1984) 906–920.
[55] N. Tsuji, Y. Suzuki, A. Matsumoto, Adamantane-containing poly(dialkyl fumarate)s with rigid chain structures, Polym. J. 51 (2019) 1147–1161.
[56] K.J. Dawson, L. Zhu, L. Yu, M.D. Ediger, Anisotropic structure and transformation kinetics of vapor-deposited glasses, J. Phys. Chem. B 115 (2011) 455–463.